ADVANCED ENGINEERING MATERIALS
www.aem-journal.com

Understanding the Room Temperature Recovery Behavior in a Ti–24Nb–4Zr–8Sn Superelastic Alloy

*Oliver G. Reed, Nicole L. Church, and Nicholas G. Jones**

Metastable β Ti–Nb-based superelastic alloys have potential uses in the biomedical and aerospace industries due to an attractive combination of properties. However, their mechanical response can be seen to vary with cycling, limiting their uptake. Furthermore, recent studies have also highlighted changes in properties under no applied stress at room temperature, with the reasons for these changes poorly understood. To investigate potential mechanisms for these changes, the superelastic behavior of Ti–2448 is studied during mechanical cycling both pre- and post-room temperature (RT) aging treatments. On cycling, there is a reduction in both σ_{SIM} and hysteresis area, consistent with behavior commonly seen in the literature. However, during RT aging, there is a rapid, time-dependent process leading to a partial recovery. In situ diffraction data indicated that this recovery is coincident with a reduction in internal stresses, the potential mechanisms for which are discussed.

1. Introduction

Ti–Nb-based alloys have the ability to reversibly transform between the body-centered cubic (bcc) β phase and the orthorhombic α″ martensite. This transformation can be thermally or mechanically induced and is both highly scalable and tuneable, giving rise to potential applications across multiple sectors including the aerospace and biomedical industries. Although the properties of these alloys may vary based on the desired application, their commercial uptake is limited by one key issue affecting all known materials of this class: a change in the thermal or mechanical response of the material with repeated transformations.[1]

In Ti–Nb-based alloys, the mechanical transformation and changes that occur during repeated loading have been widely studied.[2–8] The α″ martensite is formed on loading above a critical applied stress, σ_{SIM}, which is acutely sensitive to the alloy composition, and processing history.[9–11] During repeated loading, the magnitude of σ_{SIM} decreases, with the most dramatic changes observed within the first few cycles. Most studies agree that the transformation from β to α″ results in the generation of dislocations that form to accommodate the irrational β/α″ phase boundary.[12] It has been suggested that these dislocations, and their associated strain fields, are important for stabilizing the α″ in the microstructure, manifesting as a decrease in σ_{SIM} and in some cases retaining α″ on unloading.[2] Similar rationale has been used in the literature for other transforming systems, such as NiTi, which are similarly affected by changes in behavior following repeated cycling.[13]

However, more recently, it has been observed that the effects of repeated loading may not be permanent, with recovery in σ_{SIM} reported following heating to temperatures where dislocations become mobile.[14] At these temperatures, the rearrangement of dislocation structures could help to accommodate their associated strain fields, in order to lower the overall energy, thus returning the microstructure to a condition more comparable to the unloaded specimen.[15] However, some recovery in σ_{SIM} has also been seen after holding in ambient conditions and coincide with a decrease in the stable volume fraction of α″.[16] These effects have been shown to occur rapidly, with changes seen within an hour.[16,17] These time periods are inconsistent with the substitutional diffusional processes necessary for dislocation recovery,[18] and thus the mechanism driving this room temperature (RT) recovery is poorly understood.

A number of alternative mechanisms have been proposed to account for this behavior. Some of the first studies reporting this phenomenon suggested that these effects could be explained by the movement of point defects, via diffusion along dislocation cores, or grain boundaries.[16,17] The arrangement of these point defects was hypothesized to be influenced by the surrounding crystal structure and hence during cycling they would adopt the symmetry of the α″. During RT aging, the point defects could then readopt the symmetry of the β phase, resulting in an increase in β phase stability and hence result in an increase in σ_{SIM}. However, this argument is inconsistent with the observation of elevated levels of σ_{SIM} in samples aged without any prior deformation, and in values of σ_{SIM} that surpassed that of undeformed specimens.[5] As such, any mechanism rationalizing these effects must necessarily be independent of any requirement for prior martensitic transformation.

O. G. Reed, N. L. Church, N. G. Jones
Department of Materials Science and Metallurgy
University of Cambridge
27 Charles Babbage Road, Cambridge CB3 0FS, UK
E-mail: ngj22@cam.ac.uk

The ORCID identification number(s) for the author(s) of this article can be found under https://doi.org/10.1002/adem.202400076.

DOI: 10.1002/adem.202400076

An alternative mechanism suggested that precipitation of the isothermal omega phase, ω_{iso}, may be responsible, with an increase in ω_{iso} seen in samples following RT aging for 28 days.[5] ω_{iso} forms via diffusional processes, resulting in a Ti-rich hexagonal precipitate known to embrittle alloys and suppress the martensitic transformation.[19,20] This suppression would manifest as an increase in σ_{SIM} and would not be reliant on any prior superelastic transformation. To test this hypothesis, alloys varying in Sn content were considered,[5] as Sn is thought to be effective at suppressing ω_{iso} formation.[21] In alloys with higher Sn content, the extent of RT recovery was reduced, which would appear to support a mechanism based on ω_{iso}. Despite this, RT recovery phenomena have also been observed in other alloy systems such as NiTi, which does not form ω_{iso}.[22] As such, it seems likely that other factors may be responsible for the increases in σ_{SIM} following RT aging.

Therefore, this work considers the RT recovery behavior of a commercial Ti–Nb-based alloy (Ti–24Nb–4Zr–8Sn wt%) thought to be resistant to the low-temperature formation of ω_{iso}. The mechanical behavior of the alloy following a range of recovery intervals was studied ex situ in order to determine the time-dependency of the recovery process. These data were supplemented with in situ synchrotron radiation observations, in order to elucidate the mechanisms governing the change in properties during the RT hold.

2. Experimental Section

A commercially produced plate of Ti–24Nb–4Zr–8Sn (Ti–2448), 2 mm thick, with a measured composition of Ti–24.19Nb–3.72Zr–7.29Sn (wt%) was chosen for the present work. This alloy is well suited to this investigation as it was specifically designed to be less sensitive to the formation of the ω phase than other Ti–Nb-based alloys.[23–25] It should be noted that this material has a lower O and Sn content than that reported in other studies in the literature and, as such, may display some differences in behavior compared to these. Nevertheless, previous work on this composition has similarly shown low sensitivity to ω_{iso} even when heated to elevated temperatures.[15]

The 2 mm plate was cold rolled to 0.5 mm final thickness, equivalent to a reduction ratio of 75%. Dog bone tensile samples with a gauge section of $(0.5 \times 0.5)\ mm^2$ were produced from the rolled material by electro-discharge machining. These samples, alongside a piece for ex situ microstructural characterization, were sealed in evacuated quartz ampules, with Ta, as an oxygen getter, and solution heat treated for 5 mins at 900 °C, followed by air cooling.

Samples for microstructural characterization were ground with 5 μm SiC paper, polished using 0.04 μm colloidal silica, and buffered to pH 7. Electron channeling contrast imaging (ECCI) was utilized to assess the microstructure of the initial condition, performed using a Zeiss GeminiSEM 300. Micrographs were obtained using a backscattered electron detector at an accelerating voltage of 15 kV and a 30 μm aperture.

Ex situ mechanical testing was performed using an Instron 3367B universal testing frame with a 30 kN load cell and a 12.5 mm Epsilon contact extensometer. Mechanical cycles between a preload of 25 and 300 MPa were performed with a loading rate of 4 MPa s^{-1}. A series of 10 mechanical cycles were performed, followed by a RT age for a given period. Samples were then subjected to a further 10 mechanical cycles to assess the influence of the RT age. The hysteresis area for each cycle was taken to be the area inside the loading and unloading curves when plotted on axes of stress and strain. σ_{SIM} for each cycle was determined by extrapolating the initial linear part of the curve and determining when this deviated from the stress–strain curve by a nominal stress of 10 MPa.

A Linkam TST350 stage with a 200 N load cell was utilized for in situ mechanical testing. As with the ex situ testing, 10 mechanical cycles between 25 and 300 MPa were performed, at a displacement rate of 4 μm s^{-1}. This was followed by a 1 h hold at RT, and then a further 10 mechanical cycles. Synchrotron X-ray diffraction (SXRD) data were acquired throughout the loading and RT aging steps on the I12 beamline at Diamond Light Source.[26] The sample was illuminated with a monochromatic square beam, with a wavelength 0.1544 Å and a cross section of $(0.5 \times 0.5)\ mm^2$. The sample position remained unchanged during the RT hold, ensuring the same grains were sampled throughout, allowing direct comparisons of the volume fraction of α″ to be made. 2D diffraction patterns were collected in transmission geometry with an exposure time of 2 s (during loading) or 5 s (during the RT hold) by a CdTe 2 M Pilatus detector.[20] The beam energy and experimental geometry were calibrated using a NIST CeO_2 standard at multiple distances.[27] The 2D diffraction patterns were reduced to 1D data by integration over the entire azimuthal range using the DAWN software,[28,29] which also corrected the intensity for any change in beam current. During mechanical loading, σ_{SIM} was determined to be the stress at which the most intense α″ reflection, the $\{020\}_{\alpha''}$ peak (location indicated in **Figure 1**a), became distinguishable above the background. The $\{110\}_{\beta}$ peak during the RT age was fitted with a pseudo-Voigt function on a linear background, with the peak width calculated for each fit.

3. Results

To determine the phase constitution of the initial material, an SXRD pattern was obtained prior to testing, Figure 1a. Intense reflections consistent with a large volume fraction of the bcc β phase were present. However, a broad low intensity peak was also observed at 6.27° 2θ, indicated by the labeled arrow, which is consistent with the presence of a small volume fraction of the ω phase. This phase is often observed at RT following the solution heat treatment of metastable β alloys, with TEM studies in the literature showing that following air cooling of Ti–2448, it is the compositionally indistinct athermal variant (ω_{ath}) that forms.[10,30] The microstructure for the initial condition is shown in Figure 1b. Equiaxed grains of a single phase were observed, with the SXRD pattern indicating this phase as β. No evidence of α″ was found in either the SXRD or microscopy data, highlighting that the M_s temperature for this material was below RT.

Mechanical cycling between 25 and 300 MPa was performed to quantify the change in mechanical properties. The stress–strain curves of all 10 cycles are shown in **Figure 2**a, with all cycles showing a change in gradient during loading, consistent with a martensitic transformation from β to α″. The stress at

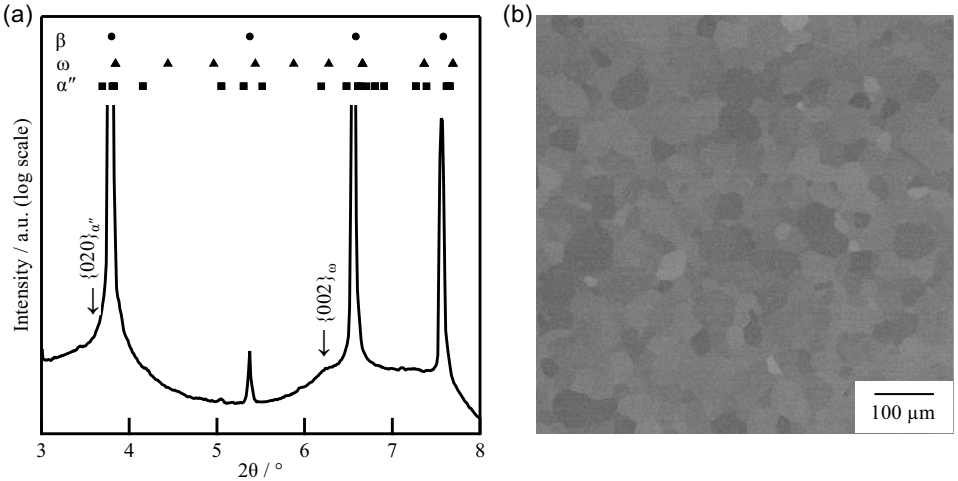

Figure 1. Microstructural characterization of Ti–2448 in its initial condition: a) SXRD pattern, with the expected peak positions of all relevant phases indicated. The broad $\{002\}_{\omega}$ peak and the initially absent $\{020\}_{\alpha''}$ peak are indicated with arrows and labelled. The small peak at 5° 2θ is an artefact that does not change position or intensity during loading. b) SEM ECCI micrograph.

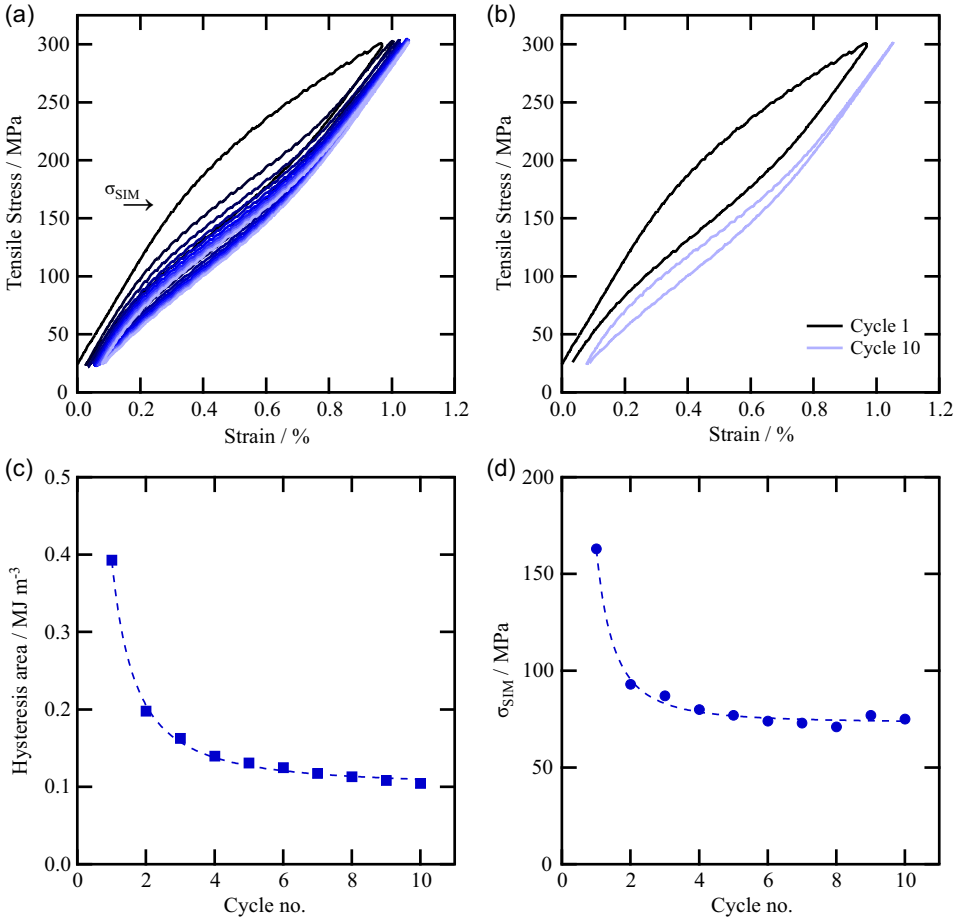

Figure 2. Mechanical testing of Ti–2448. a) 10 cycles of load and unload to a single stress, with σ_{SIM} for the first cycle indicated; b) The 1st and 10th cycle, indicating the change in behavior; c) the drop in hysteresis area during cycling; and d) the drop in σ_{SIM} during cycling, with a power law line of best fit.

which this transformation was induced, σ_{SIM}, is indicated by an arrow for the first cycle. The stress–strain curves corresponding to cycles 1 and 10 are highlighted in Figure 2b, with the different shapes of the curves indicating there was a substantial change in behavior during cycling.

Analysis of these data revealed a decrease in both hysteresis area (Figure 2c) and σ_{SIM} (Figure 2d) occurred following cycling. The decrease in these properties was found to follow a power law decay, being largest in the first few cycles. This is consistent with the cyclic degradation of Ti–2448 reported in the literature, which is sometimes referred to as functional fatigue.[2,4] It has been shown that the decay in hysteresis area and σ_{SIM} continues with repeated cycling, for a range of Ti–Nb-based alloys.[5–8]

To elucidate the effect of an RT aging treatment, a second set of 10 cycles to 300 MPa was performed on the same sample following 24 h under ambient conditions. These data (cycles 11–20) are shown in **Figure 3**a, offset by 0.2%, alongside the original 10 cycles. Figure 3b presents the 10th cycle of the initial test, alongside the 1st cycle after a 24 h RT age (cycle 11), again offset by 0.2%. The 11th cycle showed a larger hysteresis and greater σ_{SIM} than the 10th cycle, which contrasts with functional fatigue behavior. This demonstrates that the RT age is influencing the ease of transformation in the material. The values for cycle 11 remained below that of cycle 1, indicating this effect is not sufficient to return the sample to the initial condition in 24 h.

Further changes in behavior were observed in the second set of 10 cycles, with a decrease in hysteresis area and a drop in σ_{SIM}, indicative of additional functional fatigue. Both properties were tracked across all 20 cycles and are shown in Figure 3c,d, respectively. It can also be seen that although there was an initial increase of both properties following aging, this effect was not permanent and, after just a few cycles, both return to the values they were before aging.

An increase in hysteresis area and σ_{SIM} following an RT age has previously been reported in the literature.[16,17] Despite this, to the best of the authors knowledge, there have been no studies that have considered whether this effect can be repeated following multiple holding periods. To this end, the same sequence of a 24 h age at RT, followed by 10 mechanical load cycles, was performed twice more on this sample. The hysteresis area and σ_{SIM} for these 40 cycles are shown in **Figure 4**a,b, respectively. After each 24 h age, there is an increase of both hysteresis area and σ_{SIM}, followed by a rapid decrease to a baseline value. This indicates that recovery can occur multiple times after cycling.

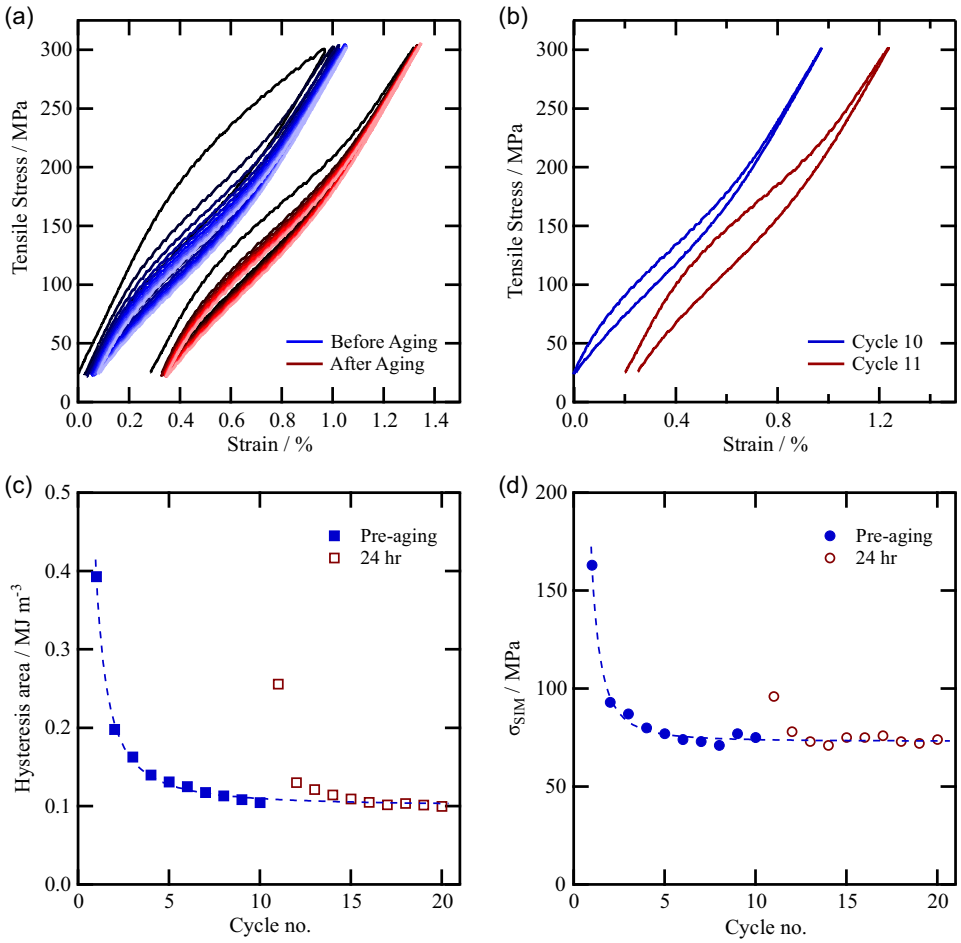

Figure 3. The effect of a 24 h RT age. a) stress–strain curve showing 10 mechanical cycles before and after aging, with those after being offset by 0.2%; b) the 10th cycle before aging, alongside the first cycle after aging (cycle 11) showing the effect the aging has; c,d) the variation in stress hysteresis and σ_{SIM}, respectively, during mechanical testing, both before and after the aging. The dotted line shows an extrapolated power law fit from the first 10 cycles.

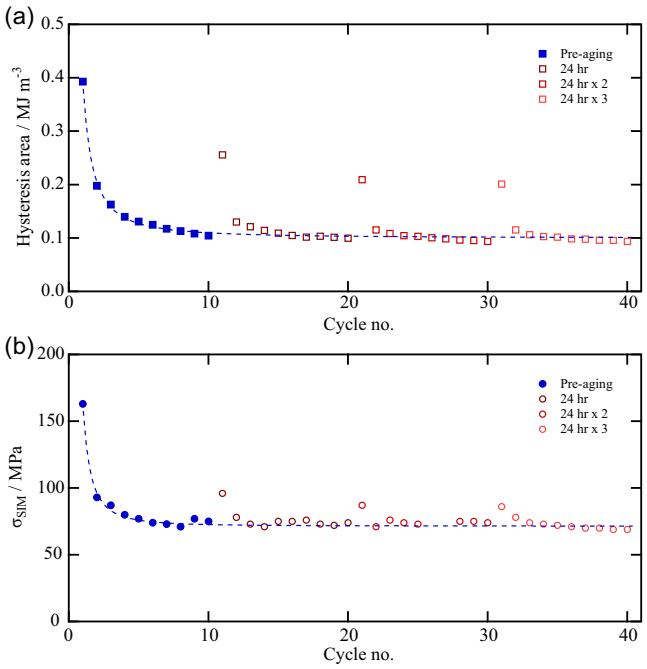

Figure 4. The variation in a) the hysteresis area and b) σ_{SIM} during repeated mechanical loading and 24 h RT holds. The dotted line shows an extrapolated power law fit from the first 10 cycles.

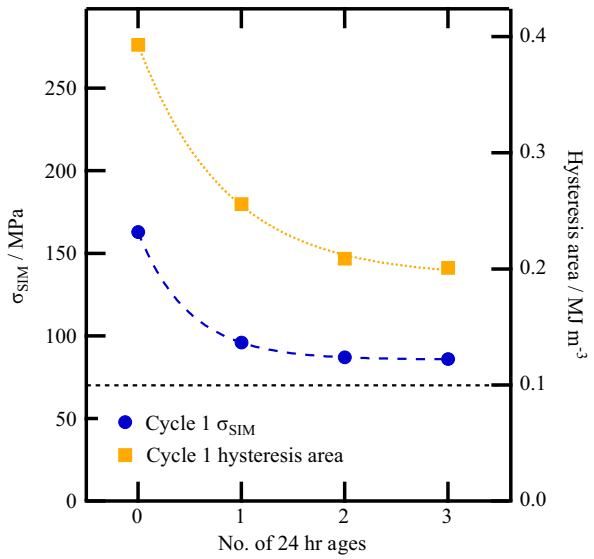

Figure 5. The value of hysteresis width (right *y* axis) and σ_{SIM} (left *y* axis) in cycle 1 against the number of sequences of 10 mechanical cycles and a 24 h RT age. The value of σ_{SIM} and hysteresis area for cycle 10 is shown by the fine black dashed line.

However, the values of σ_{SIM} and hysteresis area in the first cycle after each 24 h hold were not constant. The value of each property in this first cycle is plotted against the number of 24 h holds that have been performed, as shown in **Figure 5**. This indicates that both properties decreased with the number of 24 h holds performed, indicating that the hold is becoming less effective in recovering the properties. Furthermore, σ_{SIM} and hysteresis area both decay at comparable rates, indicating that the mechanisms governing this change may be linked.

To identify whether the mechanism governing this RT recovery is time dependent, the same sequence of 10 mechanical cycles followed by an RT age was repeated using new samples for multiple different aging times. The magnitude of σ_{SIM} and the hysteresis area of the first cycle following an RT age of different lengths are shown in **Figure 6**. Dashed lines indicate the value of σ_{SIM} and hysteresis area of the initial material (coarse red) and after 10 mechanical cycles (fine black). The RT age for 1 h shows considerable recovery, demonstrating that the mechanism driving this change in σ_{SIM} and hysteresis area must be able to happen quickly at RT. Further recovery in both properties is observed when holding for longer periods, indicating a time-dependent process. However, beyond ≈24 h, there appears to be a plateau in the recovery of both σ_{SIM} and hysteresis area, which suggests there is a limit to the amount of recovery possible. Both properties show a similar time dependence which again suggests that the effects may be linked.

Ex situ cycling following aging highlights that there are sufficient changes in the material even within an hour at RT to result in an alteration of the macroscopic tensile properties. To provide more information about these changes, the same sequence of mechanical cycling interspersed by a 1 h RT age was performed in situ using synchrotron radiation.

From the SXRD patterns, the point at which α″ is formed on loading, σ_{SIM}, may be determined by considering the stress at which the α″ peaks can be discerned above the baseline. **Figure 7** shows σ_{SIM} for each cycle before and after the 1 h age. The initial value of σ_{SIM} and the value that σ_{SIM} recovers to agree within 20 MPa of those measured ex situ, with the small discrepancy likely due to sample-to-sample variation and the use of a different method of measuring σ_{SIM}. Critically, σ_{SIM} decays

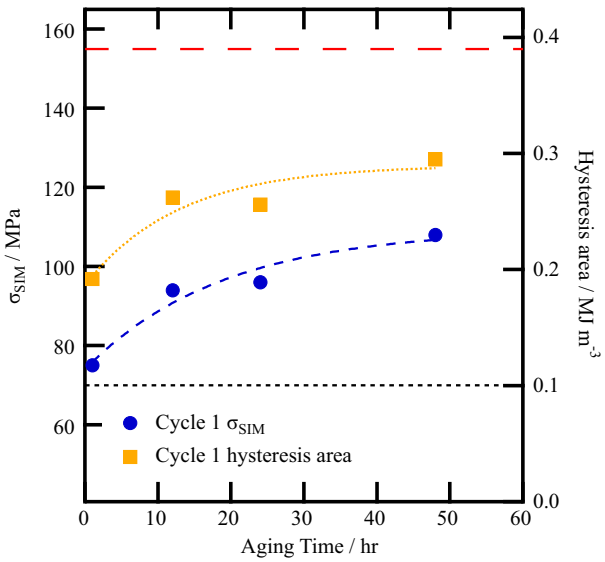

Figure 6. The effect of aging time at RT on the amount of recovery in σ_{SIM} and hysteresis area. The values of σ_{SIM} and hysteresis area for cycle 1 are shown by the coarse red dashed line and the values for cycles 10 are shown by the fine black dashed line.

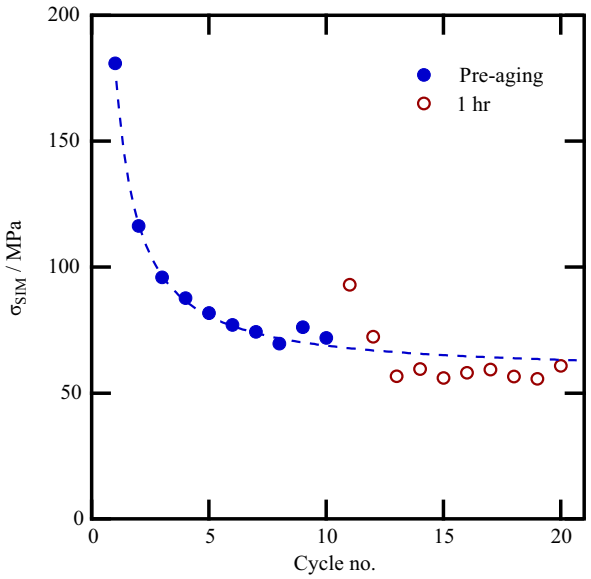

Figure 7. The effect on σ_{SIM} of mechanical cycling, interrupted by a 1 h age at RT. The dotted line shows an extrapolated fit from the first 10 cycles.

during mechanical cycling and increases following an RT hold, consistent with the ex situ data.

To determine the changes occurring in the material, synchrotron patterns were continuously obtained during the 1 h hold. In the initial condition, only the $\{110\}_\beta$ peak was present within a 2θ range of 3.5° to 3.9°, as indicated in **Figure 8**a. However, following the first 10 cycles, an additional peak was observed. This highlights that there was some retention of α″ in the microstructure following cycling, consistent with previous literature on this alloy.[2] Interestingly, the intensity of the α″ peak was found to decrease during the 1 h hold at RT, implying that the volume fraction of α″ had reduced.

Recent literature has suggested the formation of ω_{iso} as being a possible cause for the recovery of σ_{SIM} at RT.[5] Therefore, the potential evolution of the most intense unique ω reflection was also considered, with the broad $\{002\}_\omega$ peak in the initial condition, following 10 cycles and after an RT age shown in Figure 8b. The ω_{iso} has been shown to form precipitates of a similar size to the initial ω_{ath} in Ti–2448, and hence any formation of ω should be detectable as a change in an ω reflection peak profile.[10] However, there was no evidence of a change in the $\{002\}_\omega$ peak profile, indicating that the volume fraction of ω phase was unchanged during the RT hold, meaning this cannot be responsible for the changes in mechanical properties in this case. Furthermore, no extra reflections were seen after aging, indicating that there has not been formation of any other precipitates or phases during the age.

The SXRD data can also give an indication of other changes that occur in the material, which may be responsible for the increase in σ_{SIM} following aging at RT. To this end, the evolution of the $\{110\}_\beta$ peak was monitored during the 1 h hold. The width of the fitted peak was found to decrease with aging time, as shown in **Figure 9**. The width of the peak during an isothermal hold may decrease due to either an increase in grain size or a reduction in type III internal strains. The same volume of material is being sampled during data collection, and the β grains are already sufficiently large that any small changes would have no noticeable effect on the peak width, and consequently, the change in peak width can only be consistent with a reduction in internal type III strains. Such strains are intragranular, creating local distortions in crystal structure, which result in a greater angular range over which Bragg's law is obeyed and hence peak broadening in the corresponding diffraction pattern.[31–33] Type III strains arise due to defects, such as dislocations, and hence, a material with a greater dislocation density will have larger internal strains and stresses.[31–33]

4. Discussion

During a hold at room temperature, there is a change in functional properties, with σ_{SIM} and hysteresis loop area increasing.

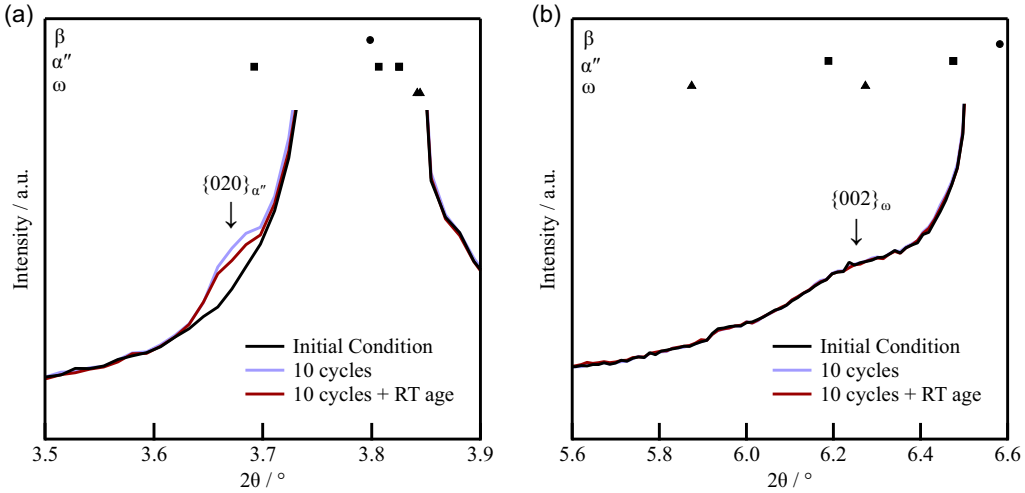

Figure 8. The evolution of phase constitution during mechanical testing and a subsequent hold at RT. a) the $\{020\}_{\alpha''}$ peak and b) the $\{002\}_\omega$ peak. Both are plotted on linear intensity scales.

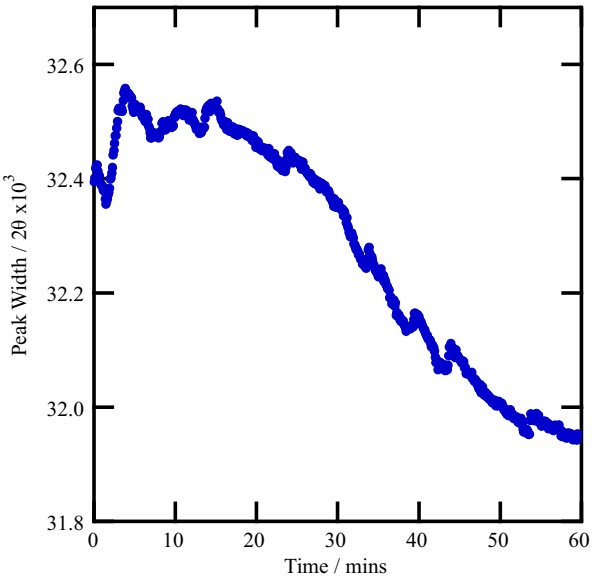

Figure 9. The change in width of the $\{110\}_\beta$ peak during a 1 h RT hold.

The increase in both properties is initially quick, with significant changes within 1 h. The process is time dependant, with a larger increase for longer aging times, up to around 24 h, after which the increase in σ_{SIM} and hysteresis area plateaus. Both σ_{SIM} and hysteresis area increase at a similar rate, suggesting that the mechanism driving this recovery may be linked.

During a 1 h hold at RT in situ, after 10 cycles of deformation, SXRD patterns showed that there was a decrease in the volume fraction of α″. This indicates that there was a change in the phase stability, with the β phase becoming more stable over time with respect to the α″ phase. This increase in β phase stability means a larger applied stress is required to induce the α″ on subsequent cycling, and thus explains the increase in σ_{SIM} post RT aging. This is consistent with the conclusions reached by similar studies on RT recovery behavior.[5,16] However, the mechanisms responsible for this effect remain unclear.

There have been several theories proposed in the literature to rationalize a change in phase stability with RT aging. An early observation of RT recovery hypothesized that point defects in the material adopt the symmetry of the phase they are present in, and consequently stabilize it locally. Hence during loading, a greater fraction of the point defects adopt the symmetry of the α″, leading to an increase in α″ stability and a decrease in σ_{SIM}. When held at RT, the defects in the β phase readopt cubic symmetry leading to an increase in σ_{SIM} on subsequent cycling.[16,17] However, this theory is inconsistent with more recent work, which has shown that there can be an increase in σ_{SIM} during aging without prior deformation, and without forming α″.[5] Furthermore, the synchrotron diffraction patterns collected as part of this work indicate that some material reverts to β during the RT hold. This is inconsistent with the above theory, as any point defects in the α″ phase would not lead to a transformation to β.

An alternative theory attributed the change in phase stability to a change in composition of the transforming phase,[5] as σ_{SIM} is known to be highly sensitive to composition.[9,34–36] In Ti–Nb-based alloys, a change in composition can result from the formation of the ω_{iso} phase, which is a deleterious phase that typically forms at temperatures ≈200–400 °C.[37] This phase is compositionally distinct from the β phase, and its formation leads to enrichment of the β phase in β-stabilizing elements. Recent studies have shown that ω_{iso} can form in some Ti–Nb alloys at RT, and it has been suggested that this rationalizes the increase in σ_{SIM} following cycling[5] as well as the increased σ_{SIM} in aged virgin material. Although this theory explains the changes seen in some Ti–Nb alloys, recovery of superelastic properties during an RT hold has been reported in NiTi superelastic alloys,[16,22] which do not form the ω phase, or any similar phases at RT that may alter the composition of the transforming phase. Additionally, the alloy studied in this work, Ti–2448, which showed recovery of functional properties, is resistant to ω_{iso} formation at RT. This was confirmed through the SXRD data presented in Figure 8b, with no ω evolution observed during the 1 h hold at RT. While it is not disputed here that the formation of ω_{iso} at RT in Ti–Nb alloys will have an effect on the superelastic properties, and that in some cases may be the dominant mechanism, this theory is not sufficient to explain RT recovery behavior in all Ti–Nb alloys and other superelastic systems.

Alternatively, the mechanism driving the increase in σ_{SIM} and hysteresis area may be linked to the reason for their decrease during mechanical cycling. It has recently been suggested in the literature that the change in superelastic properties during mechanical cycling is driven by changes in internal stress.[38] The internal stress of the material includes a contribution from dislocations produced during the martensitic transformation that accommodate the irrational interface between the β and α″ phases.[12,39] On unloading, the α″ reverts to β, but the geometrically necessary dislocations that formed during loading, and their associated stress fields, remain. Hence, on subsequent loading, the macroscopic applied stress needed to induce the martensitic transformation, σ_{SIM}, is reduced, as was observed during the initial 10 cycles.[40] Eventually, the level of internal strain can build to the point where it is sufficient to locally retain α″ in the absence of an external load,[2] explaining the presence of the martensite in the SXRD pattern at the start of the RT hold. The hysteresis area and hence the energy absorbed by the material during a mechanical cycle also decreased, again as observed during the initial 10 cycles.

This work utilized in situ methods to demonstrate, for the first time, that during a 1 h hold at RT, the width of the $\{110\}_\beta$ peak decreased. As discussed earlier, this corresponds to a decrease in type III internal stresses. In an analogous but contrasting manner to the raising of σ_{SIM} with mechanical cycling, a lowering of the internal stresses during an RT age stabilizes the β phase with respect to the α″ phase,[15] leading to an increase in σ_{SIM} and hysteresis width. Such a reduction in internal stress is not limited to the Ti–Nb system and could be applicable to RT aging in other superelastic systems, although further work would need to be undertaken to demonstrate this. At RT, there is insufficient thermal activation for dislocations to travel long distances and annihilate. However, it is conceivable that the stress fields associated with dislocations may relax, reducing the internal stress and so reducing the stability of the α″. An increase in σ_{SIM} following mechanical deformation has been shown to be possible

when heating to temperatures as low as 200 °C for very short periods of time, and complete recovery of the transformation behavior is possible following heating to 350 °C.[14] Both observations were reported to be due to the reduction in internal stresses following these heat treatments.[14]

Due to the high levels of stress surrounding the dislocation structures, there will be a significant driving force for their strain fields to interact with solute atoms, as such interactions decrease the associated stresses. This is analogous to Cottrell atmospheres of carbon in steels where, at RT, rapidly diffusing interstitial carbon atoms migrate to dislocation cores, to reduce the overall energy of the system, by reducing both the strain field of the carbon atom and the dislocation.[41–43] In Ti–2448, the change in superelastic properties during an RT age has been shown to occur quickly, with significant changes within an hour, meaning this effect is likely to be dominated by interstitial atoms, as with Cottrell atmospheres. Although there is negligible carbon in this alloy, previous compositional analysis has highlighted significant amounts of the interstitials oxygen and nitrogen. The diffusion of these interstitials in β Ti alloys at RT has not been measured, but by extrapolating from data obtained at high temperature,[44–46] and by considering the diffusion of interstitials in other bcc systems at low homologous temperatures,[41,47,48] it should be possible for these species to diffuse across length scales on the order of the grain size within an hour. Hence, oxygen and nitrogen within Ti–2448 would have sufficient mobility to migrate to regions of high strain during an RT age and lower the internal stresses.

This is not the only mechanism that may operate to reduce internal stresses during an RT hold. Due to the large density of dislocations generated at the β-α″ interface, there would be large internal stresses in the vicinity of these features, and therefore a large driving force for dislocation rearrangement. Despite the lower temperatures and thermal energy available, which limit diffusion over long length scales, these large driving forces may allow for a level of recovery over short length scales. Furthermore, it is reported that other processes requiring short-range diffusion, such as the formation of ω_{iso}, can occur at RT in Ti–Nb alloys.

It was also shown in this study that recovery is possible multiple times, with the values of σ_{SIM} and hysteresis area increasing during a second RT age after a second set of mechanical cycles. However, the recovery after the second set of mechanical cycles is smaller than that after the initial set. These results are all consistent with an interstitial-based stress reduction mechanism. During each hold, the interstitials migrate to the regions of highest strain in the sample, lowering the overall stress and leading to recovery. The second set of mechanical cycles has inflicted more damage on to the sample, and there are a limited number of interstitials, resulting in less effective relaxation of internal stresses and less recovery of σ_{SIM} and hysteresis width. An interstitial-based argument also explains the plateau in recovery with aging time, with the interstitials reaching a state where they are all sat at low energy positions, which does not necessitate having relaxed all of the internal stresses.

Finally, it was shown in the literature that there may be an increase in σ_{SIM} during RT aging, following a heat treatment, without prior deformation. It was proposed that this increase was due to formation of ω_{iso}. However, as similar effects can be seen independently of any ω_{iso} phase formation in the present study, any such mechanism cannot be occurring in isolation. As such, it must also be considered that changes in internal stress levels are also playing a role. In the literature studies, the samples were quenched post heat treatment, which may introduce these internal stresses into the material.[10] This would have a similar effect as mechanical cycling, with a lower value of σ_{SIM} and hysteresis area relative to an air-cooled sample.[10] The subsequent relaxation of the internal stresses, by the movement of interstitials, could contribute to an increase in σ_{SIM} and hysteresis area, with any rise in σ_{SIM} exacerbated by the formation of ω_{iso}.

5. Conclusion

This study investigated the effect of a series of RT ages on the superelastic properties of Ti–2448. The changes in hysteresis width and σ_{SIM} were assessed before and after RT aging, through ex situ mechanical testing. The crystallographic changes occurring in the material during the RT age were studied using in situ characterization techniques, in order to elucidate a mechanism for the changes in properties observed.

Ti–2448 showed a decrease in σ_{SIM} and hysteresis width during mechanical cycling. This functional fatigue was due to an accumulation of internal stress, stabilizing the α″ with respect to the β phase. During an RT age, there was a recovery in σ_{SIM} and hysteresis width, coinciding with a reduction in the volume fraction of α″. This was shown to occur independently of any additional phase formation, highlighting that current theories which rationalise this recovery in superelastic properties are incomplete, and cannot explain similar behavior in the present alloy.

Novel in situ synchrotron studies demonstrated, for the first time, that the peak width of the β phase decreased during an RT hold. This can only be explained by a reduction of type III internal stresses. This reduction is believed to be dominated by the diffusion of interstitial atoms to sites of high strain, mutually accommodating their stress fields and lowering the overall strain energy of the system.

Acknowledgements

O.G.R. would like to acknowledge support from the EPSRC and Rolls Royce through the provision of grant 2738194. N.L.C. would like to acknowledge support from the EPSRC and the Defence Science and Technology Laboratory through the provision of an Industrial CASE studentship (EP/R511870/1). Beam time was provided by Diamond Light Source under MG33585.

Conflict of Interest

The authors declare no conflict of interest.

Author Contributions

O.G.R.: Conceptualization, methodology, formal analysis, investigation, validation, writing—original draft, and visualization. N.L.C.: Conceptualization, methodology, formal analysis, investigation, validation, writing—original draft, and supervision. N.G.J.: Conceptualization,

methodology, formal analysis, investigation, validation, resources, writing—original draft, supervision, project administration, and funding acquisition.

Data Availability Statement

The data that support the findings of this study are openly available in University of Cambridge repository at https://doi.org/10.17863/CAM.104632, reference number 1574525.

Keywords

cyclic behavior, martensitic transformations, superelasticity, Ti–Nb

Received: January 11, 2024
Revised: February 28, 2024
Published online:

[1] J. Mohd Jani, M. Leary, A. Subic, M. A. Gibson, *Mater. Des.* **2014**, *56*, 1078.
[2] N. Church, C. Talbot, L. Connor, S. Michalik, N. Jones, *Materialia* **2023**, *28*, 101719.
[3] L. Héraud, P. Castany, M. F. Ijaz, D. M. Gordin, T. Gloriant, *J. Alloys Compd.* **2023**, *953*, 170170.
[4] R. Yang, Y. L. Hao, S. J. Li, *Biomedical Engineering, Trends in Materials Science*, Books on Demand, Germany **2011**, p. 225.
[5] Y. Al-Zain, Y. Sato, H. Y. Kim, H. Hosoda, T. H. Nam, S. Miyazaki, *Acta Mater.* **2012**, *60*, 2437.
[6] M. Tahara, H. Y. Kim, H. Hosoda, S. Miyazaki, *Acta Mater.* **2009**, *57*, 2461.
[7] V. A. Vorontsov, N. G. Jones, K. M. Rahman, D. Dye, *Acta Mater.* **2015**, *88*, 323.
[8] J. Coakley, K. M. Rahman, V. A. Vorontsov, M. Ohnuma, D. Dye, *Mater. Sci. Eng., A* **2016**, *655*, 399.
[9] H. Y. Kim, J. Fu, H. Tobe, J. I. Kim, S. Miyazaki, *Shape Mem. Superelasticity* **2015**, *1*, 107.
[10] N. L. Church, C. E. P. Talbot, N. G. Jones, *Shape Mem. Superelasticity* **2021**, *7*, 166.
[11] L. López Pavón, H. Y. Kim, H. Hosoda, S. Miyazaki, *Scr. Mater.* **2015**, *95*, 46.
[12] D. S. Lieberman, M. S. Wechsler, T. A. Read, *J. Appl. Phys.* **1955**, *26*, 473.
[13] R. Zarnetta, R. Takahashi, M. L. Young, A. Savan, Y. Furuya, S. Thienhaus, B. Maaß, M. Rahim, J. Frenzel, H. Brunken, Y. S. Chu, V. Srivastava, R. D. James, I. Takeuchi, G. Eggeler, A. Ludwig, *Adv. Funct. Mater.* **2010**, *20*, 1917.
[14] N. L. Church, C. E. P. Talbot, L. D. Connor, S. Michalik, N. G. Jones, *Mater. Sci. Eng., A* **2024**, *889*, 145791.
[15] N. L. Church, C. E. P. Talbot, J. R. Miller, L. D. Connor, S. Michalik, N. G. Jones, *Acta Mater.* **2023**, *255*, 119066.
[16] J. Ma, I. Karaman, H. J. Maier, Y. I. Chumlyakov, *Acta Mater.* **2010**, *58*, 2216.
[17] J. Ma, I. Karaman, Y. I. Chumlyakov, *Scr. Mater.* **2010**, *63*, 265.
[18] A. A. Kohnert, L. Capolungo, *npj Comput. Mater.* **2022**, *8*, 104.
[19] Y. Zheng, T. Alam, R. E. A. Williams, S. Nag, R. Banerjee, H. L. Fraser, in *Proc. of the 13th World Conf. on Titanium*, John Wiley & Sons, New Jersey **2016**, p. 559.
[20] J. C. Williams, B. S. Hickman, H. L. Marcus, *Metall. Trans.* **1971**, *2*, 1913.
[21] S. Cai, L. Wang, J. E. Schaffer, J. Gao, Y. Ren, *Mater. Sci. Eng., A* **2019**, *743*, 764.
[22] M. C. M. Rodrigues, G. C. Soares, L. d. A. Santos, *Materials Science Forum*, Trans Tech Publications Ltd, Switzerland **2018**, p. 380.
[23] Y. L. Hao, S. J. Li, S. Y. Sun, C. Y. Zheng, R. Yang, *Acta Biomater.* **2007**, *3*, 277.
[24] Q. Li, M. Niinomi, M. Nakai, Z. Cui, S. Zhu, X. Yang, *Mater. Sci. Eng., A* **2012**, *536*, 197.
[25] M. F. Ijaz, H. Y. Kim, H. Hosoda, S. Miyazaki, *Scr. Mater.* **2014**, *72–73*, 29.
[26] M. Drakopoulos, T. Connolley, C. Reinhard, R. Atwood, O. Magdysyuk, N. Vo, M. Hart, L. Connor, B. Humphreys, G. Howell, S. Davies, T. Hill, G. Wilkin, U. Pedersen, A. Foster, N. De Maio, M. Basham, F. Yuan, K. Wanelik, *J. Synchrotron Radiat.* **2015**, *22*, 828.
[27] M. L. Hart, M. Drakopoulos, C. Reinhard, T. Connolley, *J. Appl. Crystallogr.* **2013**, *46*, 1249.
[28] J. Filik, A. W. Ashton, P. C. Y. Chang, P. A. Chater, S. J. Day, M. Drakopoulos, M. W. Gerring, M. L. Hart, O. V. Magdysyuk, S. Michalik, A. Smith, C. C. Tang, N. J. Terrill, M. T. Wharmby, H. Wilhelm, *J. Appl. Crystallogr.* **2017**, *50*, 959.
[29] M. Basham, J. Filik, M. T. Wharmby, P. C. Y. Chang, B. El Kassaby, M. Gerring, J. Aishima, K. Levik, B. C. A. Pulford, I. Sikharulidze, D. Sneddon, M. Webber, S. S. Dhesi, F. Maccherozzi, O. Svensson, S. Brockhauser, G. Náray, A. W. Ashton, *J. Synchrotron Radiat.* **2015**, *22*, 853.
[30] C. Talbot, N. Church, E. Hildyard, L. Connor, J. Miller, N. Jones, *Acta Mater.* **2024**, *262*, 119409.
[31] H. Mughrabi, *Acta Metall.* **1983**, *31*, 1367.
[32] I. Groma, *Phys. Rev. B* **1998**, *57*, 7535.
[33] J. Jiang, T. Benjamin Britton, A. J. Wilkinson, *Acta Mater.* **2015**, *94*, 193.
[34] J. I. Kim, H. Y. Kim, T. Inamura, H. Hosoda, S. Miyazaki, *Mater. Sci. Eng., A* **2005**, *403*, 334.
[35] H. Y. Kim, S. Miyazaki, *Ni-Free Ti-Based Shape Memory Alloys*, Elsevier, UK **2018**.
[36] M. Tahara, T. Inamura, H. Y. Kim, S. Miyazaki, H. Hosoda, *Scr. Mater.* **2016**, *112*, 15.
[37] B. S. Hickman, *J. Mater. Sci.* **1969**, *4*, 554.
[38] E. M. Hildyard, L. D. Connor, N. L. Church, T. E. Whitfield, N. Martin, D. Rugg, H. J. Stone, N. G. Jones, *Acta Mater.* **2022**, *237*, 118161.
[39] E. G. Obbard, Y. L. Hao, R. J. Talling, S. J. Li, Y. W. Zhang, D. Dye, R. Yang, *Acta Mater.* **2011**, *59*, 112.
[40] N. L. Church, N. G. Jones, *Mater. Sci. Eng., A* **2022**, *833*, 142530.
[41] A. H. Cottrell, B. A. Bilby, *Proc. Phys. Soc., Sect. A* **1949**, *62*, 49.
[42] J. Wilde, A. Cerezo, G. D. W. Smith, *Scr. Mater.* **2000**, *43*, 39.
[43] K. Kamber, D. Keefer, C. Wert, *Acta Metall.* **1961**, *9*, 403.
[44] F. Claisse, H. P. Koenig, *Acta Metall.* **1956**, *4*, 650.
[45] C. J. Rosa, *Metall. Trans.* **1970**, *1*, 2517.
[46] M. Song, S. Han, D. Min, G. Choi, J. Park, *Scr. Mater.* **2008**, *59*, 623.
[47] C. A. Wert, *J. Appl. Phys.* **1950**, *21*, 1196.
[48] C. Wert, C. Zener, *Phys. Rev.* **1949**, *76*, 1169.